

Geophysical Research Letters*

RESEARCH LETTER

10.1029/2024GL108545

Key Points:

- Louisiana experienced 5 months of exceptional evaporative demand and low precipitation, including a flash drought during June 2023
- Historically low flows on the lower Mississippi River in fall 2023 were accompanied by several episodes of high evaporative demand upbasin
- Basin-wide high evaporative demand coincides with low discharge near New Orleans, with a trend toward this combination since the 2019 flood

Correspondence to:

P. W. Miller,
pwiller1@lsu.edu

Citation:

Miller, P. W., & Hiatt, M. (2024). Hydrometeorological drivers of the 2023 Louisiana water crisis. *Geophysical Research Letters*, 51, e2024GL108545. <https://doi.org/10.1029/2024GL108545>

Received 29 JAN 2024
Accepted 28 APR 2024

Author Contributions:

Conceptualization: P. W. Miller
Formal analysis: P. W. Miller
Funding acquisition: P. W. Miller
Investigation: M. Hiatt
Methodology: P. W. Miller
Visualization: P. W. Miller
Writing – original draft: P. W. Miller
Writing – review & editing: M. Hiatt

Hydrometeorological Drivers of the 2023 Louisiana Water Crisis



P. W. Miller^{1,2}  and M. Hiatt^{1,2} 

¹Department of Oceanography and Coastal Sciences, Louisiana State University, Baton Rouge, LA, USA, ²Coastal Studies Institute, Louisiana State University, Baton Rouge, LA, USA

Abstract During summer and fall 2023, Louisiana experienced a historic local drought while dry conditions elsewhere in the central US withheld vital runoff from the Mississippi River, leading to below-normal discharge into the Gulf of Mexico. Thus, by late October 2023, Louisiana was gripped by two super-imposed water crises: a severe local drought and saltwater contamination in the Mississippi River channel. This study frames the development of the water emergency through the lens of flash drought using the Evaporative Demand Drought Index (EDDI). The EDDI shows south Louisiana experience a flash drought during June 2023, while the Mississippi River basin was subsequently characterized by large expanses of high-percentile EDDI in August–September 2023 shortly before the saltwater intrusion episode along the lower Mississippi River. Over the last 15 years, MRB-wide EDDI percentile has oscillated between years-long elevated and depressed states, accounting for 23.7% of the monthly discharge anomaly near New Orleans.

Plain Language Summary In 2023, Louisiana experienced one of its driest and hottest summers on record. While drought developed across the state, rain shortfalls further north led to low water levels in the Mississippi River, a major navigation corridor and drinking water source for the state. As river levels fell, seawater moved into the channel, threatening to contaminate the water supply with salt. The statewide drought, particularly in coastal Louisiana, is shown to have developed rapidly during June 2023 through a process called flash drought. Meanwhile, high evaporation rates and low rainfall upriver exacerbated Louisiana's water shortage by limiting runoff into the Mississippi River. Over the last 15 years, evaporative demand over the Mississippi River watershed varies closely with river discharge near New Orleans, and even corresponds to river conditions more closely than rainfall itself.

1. Introduction

During June–November 2023, the low-gradient Louisiana coast, accustomed to frequent flooding and damaging storm surges, experienced its *driest* hurricane season in 99 years. During this 6-month period, only 391 mm (15.39 in) of rain was recorded in Baton Rouge, LA (KBTR), the lowest total since 1924, and the embedded 83-day stretch between 6 June and 27 August was the driest such period in the city's 132-year historical record (Figure 1a). Simultaneously, record-breaking heat favored increases in evaporative demand across the state, desiccating the landscape. At KBTR, daily maximum temperatures exceeded 32.2°C (90°F) for 99 consecutive days between 7 June and 13 September 2023, with 32 of these days exceeding 37.8°C (100°F). Economic losses to the state's agriculture and forestry sectors reached \$1.69 billion during the drought (Guidry et al., 2023).

While drought was gripping the region locally, another hydrological threat was brewing further up the Mississippi River basin (MRB). In early 2023, flows down the main stem of the continent's largest river had rebounded to near normal from an anomalously low-water year in 2022 (Muñoz et al., 2023). In fact, fall 2022 flows had declined so severely that the US Army Corps of Engineers (USACE) constructed an emergency sill to prevent saltwater intrusion upriver from the Gulf of Mexico; such a barrier had only been required on three other occasions (1988, 1999, 2012). However, as Louisiana's 2023 drought developed and intensified locally, precipitation declines further upbasin once again led to severe low-water conditions in the lower Mississippi River (Figure 1b). By late July 2023, USACE again began construction on an emergency sill to impede the progression of heavier, denser saltwater up the main channel of the river for the second consecutive year. Unlike 2022, however, flows continued to decline such that by 22 September 2023 USACE modeling predicted that the saltwater wedge would overtop the emergency sill and penetrate dozens of miles upriver, contaminating the New Orleans municipal water supply (Cantrell, 2023).

© 2024. The Author(s).

This is an open access article under the terms of the [Creative Commons Attribution-NonCommercial-NoDerivs License](#), which permits use and distribution in any medium, provided the original work is properly cited, the use is non-commercial and no modifications or adaptations are made.

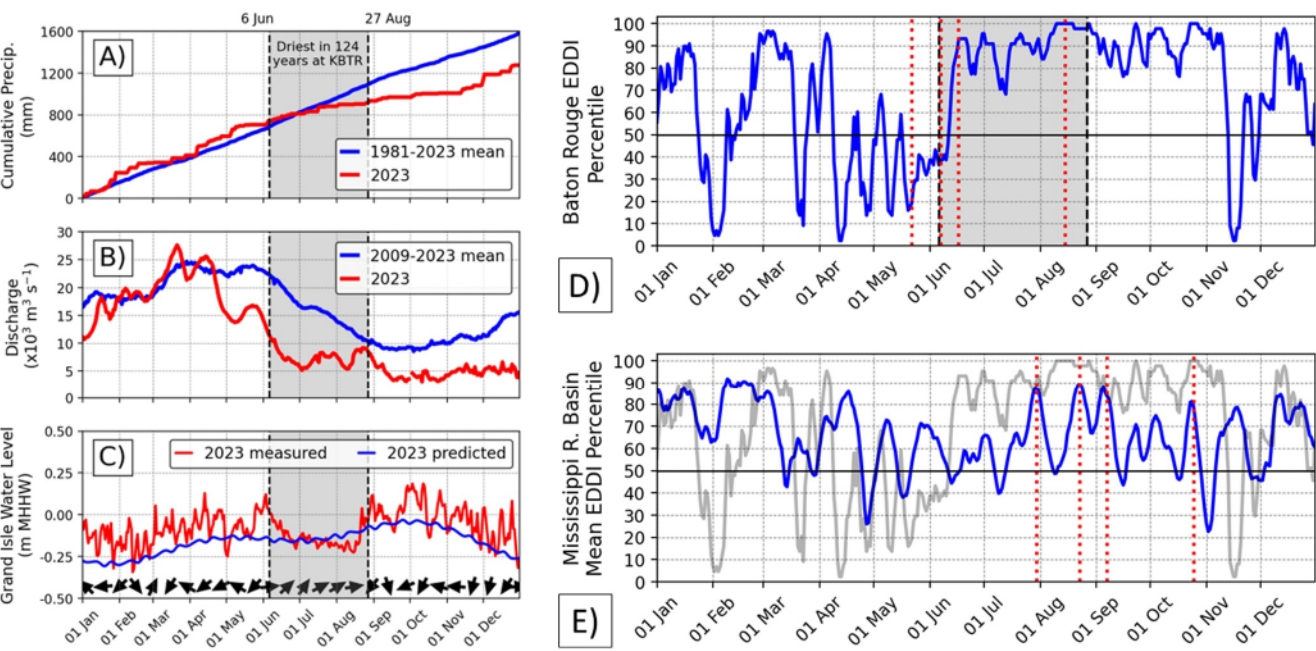


Figure 1. (a) Daily trace of 2023 (red) and normal (blue) cumulative precipitation (mm) at Baton Rouge, LA. (b) Lower Mississippi River discharge ($\text{m}^3 \text{s}^{-1}$) during 2023 (red) versus normal (blue) at Belle Chasse, LA, slightly downriver of New Orleans. (c) Weekly velocity-weighted mean wind direction (black arrow) at Grand Isle, LA, in Barataria Bay for 2023 and daily water level (m MHHW; red) versus the predicted astronomical tide (blue). (d) Seven-day Evaporative Demand Drought Index (EDDI) percentile for Baton Rouge, LA, and (e) the mean percentile for the entire Mississippi River basin. In (e), the trace from (d) is shown in light gray for comparison. Vertical red dotted lines denote dates of EDDI maps shown in Figure 2. The grayed area in (a)–(d) corresponds to the 83-day record low-precipitation stretch at KBTR.

As the New Orleans drinking water crisis illustrates, drought in coastal, river-dominated systems contains an additional layer of complexity because it serves as the terminus of the entire river system, especially those at the continent scale like the MRB. Figure 1c shows that coastal water levels in Barataria Bay, an arm of the Gulf of Mexico that lies directly south of New Orleans, dropped significantly during the intense dry spell, and the inter-daily variability became muted during this period as well. These conditions disrupt the daily cycle of inundation and exposure across Louisiana's immense wetland ecosystems. When left subaerial for prolonged periods, the marsh platform is more vulnerable to acute dieback via hypersalinity and eventually soil acidification (Alber et al., 2008; Hughes et al., 2012; Rolando et al., 2023).

The rapid shift from near-seasonal precipitation over Louisiana to well below-normal precipitation and high temperatures follows the modern paradigm of flash drought (e.g., Mo & Lettenmaier, 2015, 2016, 2020; Svoboda et al., 2002). Compared to the conventional drought paradigm which emphasizes gradually accumulating dry anomalies on longer timescales, flash drought acknowledges the more rapid onset when precipitation deficits coincide with high evaporative demand (Beguería et al., 2014; Vicente-Serrano et al., 2010). The Evaporative Demand Drought Index (EDDI), which characterizes the atmosphere's "thirst" for moisture (Hobbins et al., 2016), has been noted for its ability to detect imminent drought earlier than other drought indicators (McEvoy et al., 2016; Ramseyer & Miller, 2023), such as swift reductions in soil moisture percentile (Ford & Labosier, 2017). This study dissects Louisiana's once-in-a-century dry period through the lens of EDDI and flash drought. These same principles are then extended beyond Louisiana to understand the MRB-wide atmospheric-side forcings that ultimately yielded historically low water levels in the midst of a historically dry and hot summer.

While an increase in streamflow due to precipitation in the northern MRB in late fall 2023 ultimately spared New Orleans of salt-contaminated drinking water, the tandem hazards of the Louisiana drought and low river flows illustrate the precarious position of delta-lying cities at the mouths of large river basins (O'Donnell et al., 2024). These locations are subject to the superimposed effects of both local and distant climate conditions linked through the hydrological connectivity of their associated river. Precipitation anomalies over the river's terrestrial

watershed can yield high or low flows which can alternately inundate or contaminate either the city itself or its water supply. Simultaneously, deltaic cities also face the same agricultural and economic impacts from localized drought and floods just like anywhere else in the world. This study will help more broadly understand the development of superimposed hydrological hazards that can afflict large deltaic cities and ecosystems globally.

2. Data and Methods

Water stress is inferred using the EDDI. As detailed in Hobbins et al. (2016), the EDDI is predicated on the reference evapotranspiration (E_0) defined by the American Society of Civil Engineers (Allen et al., 2005). In this formulation, E_0 is a function of the incoming solar radiation, wind speed, temperature, and humidity. The EDDI then contextualizes accumulated E_0 over a period of interest using an empirical probability, $P(E_0)$, by comparing it against all other accumulated E_0 for the same period. For instance, to compute the 7-day EDDI ending on 30 June 2023, E_0 would be summed for the period June 24–30, 2023, and then ranked against total E_0 for June 24–30 on all other available years, n . If the June 24–30, 2023, E_0 ranked third highest out of $n = 44$ years available, then the $P(E_0) = 0.06$. The final EDDI is calculated as a transformation of $P(E_0)$ using an inverse normal approximation shown in Hobbins et al. (2016) to yield the EDDI. The EDDI generally ranges between -3 and $+3$, with positive values indicating drying and negative EDDI corresponding to wetness.

Publicly available EDDI fields are retrieved from the National Oceanic and Atmospheric Administration Physical Sciences Laboratory (NOAA, 2024) at 0.125° resolution, corresponding to the grid spacing of the National Land Data Assimilation System, version 2 (NLDAS-2), which supplies the input parameters. The repository, which begins in 1980, contains EDDI for periods as short as one week and as long as one year. To capture the evolution of the 2023 drought at the highest temporal granularity, only 7-day EDDI is considered here. The 7-day EDDI is produced daily with each field reflecting the E_0 conditions during the 7 days ending on the day of interest. A bug in the NLDAS-2 data ingestion routine between approximately August 2022 and July 2023 led to erroneously high EDDI over snow-covered areas, with residual effects lingering for several months after the bug fix. Because this error is confined to the northern MRB and was resolved early in the drought period, this study uses EDDI archive in its current form, though future work should seek an updated version of the EDDI once it is available.

An EDDI-based flash drought criteria is adopted from Pendergrass et al. (2020), which requires that the EDDI increase 50 percentiles over a 14-day period and then maintain the increase for another 14 days. Thus, all 44 years of the EDDI product are retrieved so that the 2023 percentiles can be calculated within the entire period of record. To diagnose the initiation of flash drought, every cell within each 7-day EDDI field (t_{0-6}) is compared to the next non-overlapping 7-day EDDI (t_{7-13}). Cells exceeding a 50 percentile increase in their respective EDDIs across the 14-day period (i.e., $t_{7-13} - t_{0-6}$) are then also compared to the next non-overlapping EDDI (i.e., $t_{14-20} - t_{0-6}$) and then the next (i.e., $t_{21-27} - t_{0-6}$). If the 50-percentile increase is sustained across all three comparisons, then that location is determined to have experienced a flash drought between t_0 and t_{27} .

In order to characterize the sequence of hydrological processes beginning upbasin and cascading downriver, daily precipitation and Mississippi River discharge are also retrieved. Daily precipitation is provided by the Climate Hazards Center InfraRed Precipitation with Station data (CHIRPS2) product, a satellite-based 0.05° gridded product beginning in 1981 (Funk et al., 2015). Daily discharge data are collected from the Belle Chasse, LA, river gage downstream of New Orleans, LA, operated by United States Geological Survey (Station 07374525), which began recording in 2009 (USGS, 2024). Because Mississippi River discharge and mean precipitation over the MRB exhibit seasonal cycles, which can dominate inter-monthly variability, the seasonal signal is removed from each variable prior to analysis. MRB precipitation (Belle Chasse discharge) is de-seasonalized with using a fourth- (fifth-) order polynomial function, which captures each monthly average with a mean absolute error of 7.0% (1.6%).

3. Results

3.1. Louisiana Drought Development

Louisiana rainfall was relatively typical from January through April 2023 (Figure 1c). On 1 May 2023, year-to-date rainfall was only -1.4% below normal statewide and $+15\%$ above normal in Baton Rouge. However, by 1 June, the first signs of drying began to materialize. Statewide year-to-date deficits had grown to -7.2% , while the

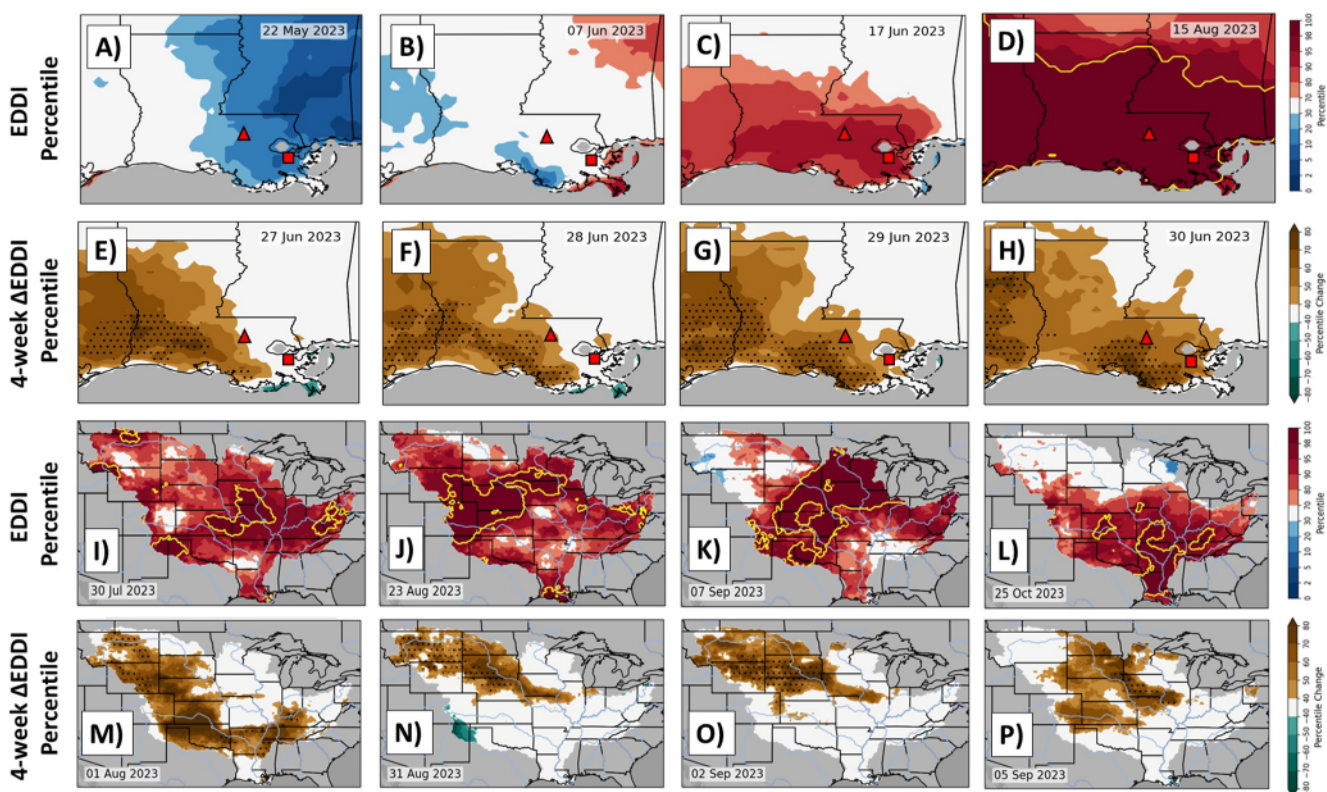


Figure 2. (a–d) Evaporative Demand Drought Index (EDDI) percentile with the 98th percentile contoured in gold and (e–h) 4-week EDDI percentile change over Louisiana. The locations of Baton Rouge (triangle) and the Belle Chasse river gage (square) are denoted in red, and cells that satisfied the flash drought criteria during the 4 weeks ending on the date shown are stippled. (i–p) Same as (a–h) but for the entire Mississippi River basin. Warm (cool) hues indicate dry (wet) anomalies.

Baton Rouge rainfall surplus had decreased to +6.9% amid a 14-day dry period. By the end of summer, statewide precipitation shortfalls had reached –14.2% and –21.3% by 1 August and 1 September, respectively, and –8.3% and –16.5% in Baton Rouge. Precipitation deficits only grew through much of the fall, reaching their peak negative anomaly on 9 November statewide (–27.6%) and 12 November in Baton Rouge (–27.1%) before improving through the end of the year.

The rapid accrual of the year-to-date anomaly during a consecutive four-month period yielded intense drought effects during the summer and early fall. The US Drought Monitor (USDM; Svoboda et al., 2002) first depicted “severe drought” (D2) anywhere in the state on 25 July. Though first “extreme drought” (D3) zone emerged on 8 August when 2.85% of Louisiana was assigned to this category, it grew to encompass 73.6% of the state by 29 August. Meanwhile, the area of “exceptional drought” (D4), the most intense USDM rating, was first invoked on 22 August and peaked on 14 November when 74.2% of Louisiana received this ranking.

The alarming growth of extreme drought across >70% of the state in only 3 weeks, coincided not only with the accrual of precipitation anomalies described above, but record-breaking temperatures. Between 8 and 29 August, the mean high temperature in Baton Rouge was 38.8°C (101.9°F). The record-breaking heat, in addition to the lack of rain, drove a shift in the surface energy budget toward a greater sensible and smaller latent heat flux component, which prompted high evaporative demand and desiccated the landscape. Figure 1d shows the time series of the 7-day EDDI percentile through 2023 for Baton Rouge. While EDDI had been variable for January through May, a regime shift occurred between late May and mid-June whereby the EDDI percentile climbed from the 19th on 22 May to 93rd on 17 June. Though briefly dipping to the still-high 68th percentile on 13 July, the EDDI then remained exclusively in the top quartile through early November and regularly rose above the 90th percentile for weeks at a time.

Figures 2a–2d depict the evolution of the May-to-June regime shift spatially across the state. Low EDDI percentiles (i.e., wetter-than-normal conditions) characterized most of southeast Louisiana on 22 May (Figure 2a),

with near-neutral EDDI elsewhere. On 7 June (Figure 2b), Baton Rouge EDDI rose marginally to the 39th percentile before surpassing the 93rd percentile only 10 days later (Figure 2c) and peaking spatially on 15 August when nearly the entire state exceeded its 98th percentile (Figure 2d). The 54-percentile increase in EDDI between 7 and 17 June satisfies the rapid-shift criterion of the flash drought definition, but a brief decline in EDDI the following week (Figure 1d) spoiled the two-week maintenance criterion.

Though Baton Rouge narrowly missed the Pendergrass et al. (2020) flash drought definition, the event does conceptually embody the flash drought paradigm, and a metric that identifies rapid drying by standardizing both evaporative demand and its fluctuations (e.g., Christian et al., 2019) may have determined otherwise. In fact, many locations in south Louisiana did satisfy both criteria during this period. Figures 2e–2h shows the flash drought outbreak across east Texas and south Louisiana that began on 31 May–3 June and concluded 27–30 June. Because the “flash” component to flash drought only references rapid onset, the “conclusion” of the flash drought outbreak in Figures 2e–2h did not mark the conclusion of the drought but only its transition to conventional drought.

3.2. Low Flows on the Lower Mississippi River and MRB Hydrometeorology

While regional drought crippled farming, ranching, and forestry in south Louisiana (Guidry et al., 2023), similar dynamics were operating on a broader scale further upbasin, where low precipitation and high evaporative demand yielded low water levels in the Mississippi River during summer and fall. Across the MRB, precipitation during 2023 was relatively typical with year-to-date anomalies generally constrained to within $\pm 5\%$. Precipitation deficits peaked at -6.1% on 9 June before recovering to normal by mid-August. However, MRB-wide deficits once again accumulated to -5.5% on 20 September, a couple days before USACE first predicted low flows would lead to saltwater contamination at Belle Chasse, LA. While the MRB-wide precipitation anomalies are much smaller than those in Louisiana during summer and fall 2023, the vast area captured by the MRB means that even a -5% year-to-date precipitation anomaly could translate into thousands of cubic meters of lost surface and subsurface runoff that would have normally flowed into the Mississippi River.

Like Louisiana, large areas of the MRB were characterized by periods of exceptional evaporative demand during summer and fall 2023. The mean EDDI percentile for the MRB (i.e., the mean of all individual-cell percentiles) is shown in Figure 1e, which resided above the 50th percentile on 307 of 365 days during 2023. The mean EDDI percentile even exceeded the 80th between 6 February and 6 March. These late winter and early spring high-evaporative-demand conditions across the entire basin likely contributed to the precipitous decline in discharge at Belle Chasse that began in late April (Figure 1b). While EDDI across the MRB moderated by the end of spring, the mean percentile spiked above the 80th again on four separate occasions between July and October. Figures 2i–2l depicts the distribution of EDDI across the MRB during each of these events. In each case, large areas of the MRB exceeded their 98th EDDI percentile. Importantly, the high EDDI percentiles in Louisiana did not contribute significantly to the MRB mean for the first three of these events (30 July, 23 August, 7 September). The semi-persistent high EDDI conditions between 28 July and 8 August, during which time the basin averaged the 73rd percentile, fueled the low-water levels at Belle Chasse in late October 2023 that threatened New Orleans with saltwater contamination.

Similar to Louisiana, the high-EDDI pulses upbasin occurred quite rapidly and constituted flash drought in many locations within the Missouri River watershed. Figure 2m shows the four-week EDDI percentile difference ending on 1 August, during which significant portions of Oklahoma and southern Kansas experienced $>80\%$ -percentile reversals. Flash drought, however, was confined to Montana and Wyoming as well as a small pocket along the Ohio River in Kentucky. A larger flash drought outbreak climaxed several weeks later between 31 August and 5 September (Figures 2n–2p) when parts of South Dakota, Nebraska, Kansas, and Iowa completed a rapid-drying cycle that began 3–9 August.

Anecdotally, the high mean EDDI percentiles (i.e., drier-than-normal conditions) across the MRB (Figure 1e) corresponded to periods of low discharge (Figure 1b) with some lag. Figures 3a–3c examines the long-term consistency of this relationship using the monthly mean-MRB EDDI percentile, mean MRB precipitation anomaly, and mean discharge anomaly at Belle Chasse. The three emergency sill episodes during the period of record in 2012, 2022, and 2023 are all characterized by a mean EDDI percentile above 50 and negative precipitation anomalies coincident with and preceding the sill construction. In contrast, exceptional high-flow

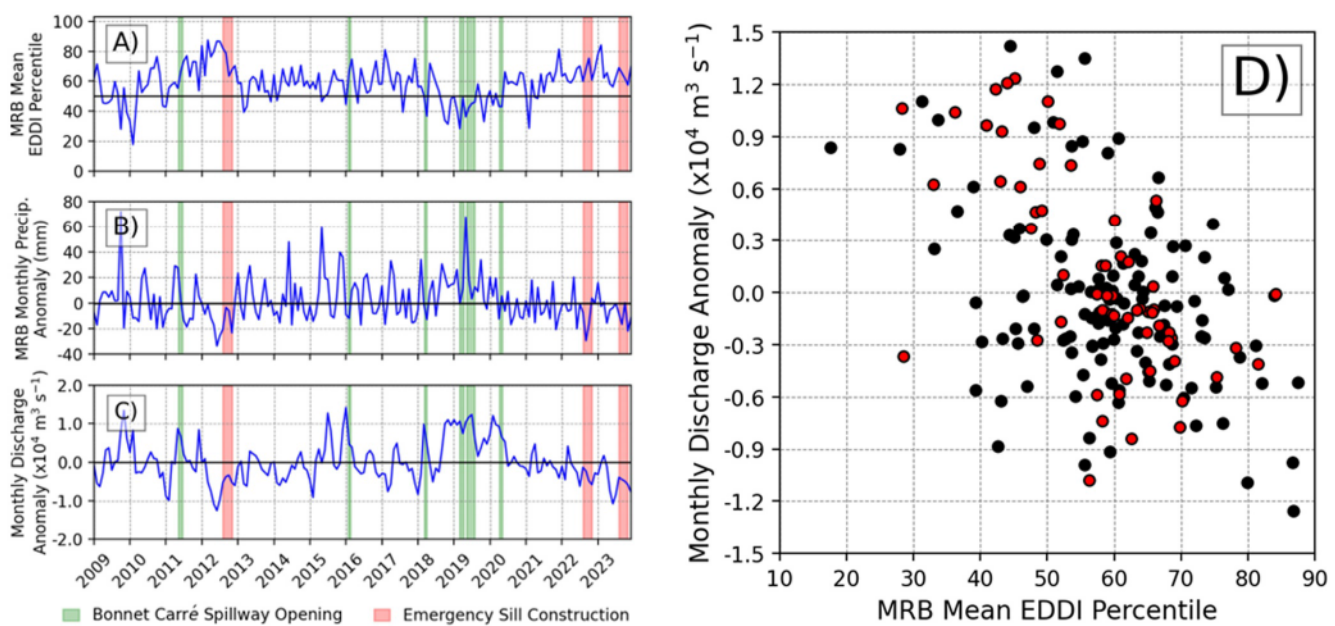


Figure 3. Time series of the monthly (a) mean Evaporative Demand Drought Index percentile and (b) deseasonalized precipitation (mm) for the entire Mississippi River basin as well as (c) the deannualized discharge at Belle Chasse between 2009 and 2023, the period of record for discharge measurements. Periods of Bonnet Carré spillway openings (green) and emergency sill construction (red) are denoted. (d) Scatterplot of data in (a) versus (c). Points during the period 2019–2023 are shown with inner red fill.

periods, which required the operation of the Bonnet Carré spillway to prevent flooding to New Orleans, are associated with positive precipitation anomalies, but not necessarily low EDDI percentiles.

Figure 3d expresses the data points in Figures 3a and 3c as a scatterplot, showcasing two apparent EDDI regimes. High monthly EDDI percentiles are generally coupled with negative discharge anomalies while low EDDI percentiles correspond with positive discharge anomalies. In fact, the mean MRB EDDI percentile explains 23.7% of the variability in the Belle Chasse monthly discharge anomaly (i.e., $R^2 = 0.237$), which is remarkable considering that precipitation only explains 10.0% nor does the EDDI incorporate any precipitation data. MRB precipitation explains 16.4% of the discharge variability when lagged by 1 month, whereas EDDI is most strongly associated to discharge with no lag. Figures 3a–3c shows that following the historic 2019 Mississippi River flood and longest-ever Bonnet Carré spillway opening, a period of higher EDDI percentiles, negative precipitation anomaly, and below-average discharges has followed. During this drier period of stronger evaporative demand across the basin, EDDI has been even more strongly correlated with the discharge anomaly, explaining 40.2% of the post-2019 variation at Belle Chasse (Figure 3d).

4. Discussion

Though the Baton Rouge precipitation shortfalls alone were sufficient to indicate drought conditions during 2023, the EDDI better captured the superimposed effect of record-breaking temperatures and below-normal precipitation. While the year-to-date precipitation in Baton Rouge was only 1.9% below normal on 1 July, Figures 2e–2h shows that neighboring grid cells had already experienced flash drought by that point. By August 2023, coincident with the USDM's first upgrade to "extreme drought," the LSU agricultural extension first surveyed the state's beef cattle and hay producers for economic losses (Guidry et al., 2023). Reports from these sectors indicated that June–August damages ranged from \$135.8 to \$290.9 million due to death loss, forced liquidation, reduced sale weight, abortions, and reduced forage production and stocking rate (Guidry et al., 2023).

In addition to the EDDI's advantages over precipitation alone as an indicator of the Louisiana drought, it also demonstrated a strong long-term relationship with Mississippi River discharge in contrast to MRB-mean precipitation. Admittedly, the type (i.e., snow vs. rain) and distribution of precipitation within the basin (e.g., van der Wiel et al., 2018), as well as evaporative loss (e.g., Twine et al., 2005), significantly complicate the relationship to Belle Chasse discharge and likely impede the simple regression analysis from detecting a stronger relationship.

However, the EDDI, not only more strongly corresponds to discharge, but it does so with no lag. Whereas Wiman et al. (2021) demonstrated that enhanced MRB evapotranspiration has driven centuries-long declines in Mississippi River discharge in the past, the seasonal-scale maintenance of this relationship is valuable for future river forecasting efforts.

By extension, Figure 3 also reveals what may be multi-year oscillations in evaporative demand that have important implications on discharge. Accounting for seasonality, the EDDI, precipitation, and discharge experience multi-year phases of elevated and depressed states. While several studies have linked Mississippi River high- and low-flow periods to phases of El Niño-Southern Oscillation (Liang et al., 2014; Muñoz & Dee, 2017; Muñoz et al., 2023) and the North Atlantic Oscillation (Turner, 2022), evaporative demand may be a mechanism by which ENSO exerts its influence. For instance, 2018–2020 was characterized by bottom 50% EDDI, above average monthly rainfall, and anomalously high discharges. However, following the peak of this pluvial phase in 2019, basin-wide EDDI has trended higher, while precipitation and discharge has trended lower. While not shown in Figure 3, the period from 1987 to 1991, which corresponds with the first-ever emergency sill construction in 1988, was also characterized by higher monthly EDDI percentiles and negative monthly precipitation anomalies.

4.1. Considerations for River-Dominated Coastal Systems

Beyond 2023's terrestrial and riverine water pressures, the Louisiana water crisis also possessed a marine dimension that is unique to river-dominated coastal systems. Despite the near-constant presence of water, drought is nonetheless detrimental to these ecosystems because it disrupts the balance of fresh versus saltwater inputs (i.e., salinity), presenting a chemical stress to the coastal marsh (Queen, 1974; Visser et al., 2002). Further, studies have hypothesized that as salt marshes experience less rainfall and/or tidal flooding, soils oxidize and turn metal sulfides into sulfuric acid, thereby reducing soil pH (Alber et al., 2008).

In 2000, a similarly severe drought afflicted the Southeast US, including much of the Gulf Coast. During this event, over 100,000 ha of *Spartina alterniflora* in Louisiana transitioned to bare mud, a process termed "acute marsh dieback." While the 2000 dieback event coincided with one of Louisiana's most serious droughts in a century (Swenson et al., 2004), a similar dieback episode in Georgia also manifested following the driest three-year period on record (Alber et al., 2008). A subsequent meta-analysis of dieback events over the Gulf of Mexico coastlines identified evidence for a relationship to drought (Alber et al., 2008). Because an estimated 35% of Mississippi Delta wetlands, which represents 40% of the total US coastal wetland area, have vertical accretion rates insufficient to keep pace with rates of sea level rise (Jankowski et al., 2017), it is imperative to understand the mechanisms by which they are threatened.

In addition to rainfall deficits, the atmospheric circulations that suppress rainfall and drive the local drought may yield wind directions that exacerbate the low coastal water conditions and soil oxidation. Figure 1c shows that the exceptionally low water at Grand Isle, coincided with three-month period of dominant southwesterly wind directions, in stark contrast to the easterly wind regime typically present in summer (Zhang & Hu, 2021). These winds would have not only advected hot, tropical air into Louisiana, fueling the heat wave, but they would have simultaneously directed Ekman transport, the vertically integrated net movement of water perpendicular to the surface wind, offshore (Walker et al., 2005). Because Ekman drawdown would create low water levels and persistent marsh platform exposure, the same atmospheric circulations that withhold water from above may also starve the state's marshes of water from beside and below, accelerating dieback.

5. Conclusions

The 2023 Louisiana water crisis exemplifies the complexity of environmental challenges facing communities along river-dominated coastlines globally. Not only are these settings subject to local climate stresses, but they are also vulnerable to climate stresses occurring over vast swathes of continental landscape (Luo et al., 2023) through the hydrological connectivity of their associated river system. When events like drought develop locally, they can be exacerbated by similar, though distant, conditions upstream, threatening the riverine freshwater supply that normally buffers against water shortages. Moreover, both the local and upbasin drought have ramifications for downstream marine resources that can typically be neglected in continental eco-drought analyses. The 2023 Louisiana drought serves as a motivation for understanding the full gamut of coupled terrestrial-marine drought dynamics and the enormous economic and environmental problems that can arise. Critically, Louisiana's high

rates of relative sea-level rise mean that saltwater will slowly encroach more closely to south Louisiana's municipal drinking water intakes, gradually lowering the threshold for events like 2023 as time progresses.

Data Availability Statement

CHIRPS2 precipitation data are available at the Climate Hazards Center (2024). Mississippi River discharge observations from Belle Chasse, LA, data can be retrieved from U.S. Geological Survey (2024). NOAA coastal water levels at Grand Isle, Louisiana, are accessible from the Center for Operational Oceanographic Products and Services (CO-OPS) (2024), and EDDI data are hosted at NOAA (2024).

Acknowledgments

PM acknowledges support from NOAA award NA20OAR4310416, NSF award 2236655, and USGS award G23AC00476 via a subaward from the University of Oklahoma. MH acknowledges support from NSF award 2408854. Additionally, research reported in this publication was supported by the Gulf Research Program of the National Academies of Sciences, Engineering, and Medicine under award number SCON-10000883. The content is solely the responsibility of the authors and does not necessarily represent the official views of the Gulf Research Program or the National Academies of Sciences, Engineering, and Medicine.

References

Alber, M., Swenson, E. M., Adamowicz, S. C., & Mendelsohn, I. A. (2008). Salt Marsh Dieback: An overview of recent events in the US. *Estuarine, Coastal and Shelf Science*, 80(1), 1–11. <https://doi.org/10.1016/j.ecss.2008.08.009>

Allen, R. G., Walter, I. A., Elliott, R. L., Howell, T. A., Itenfisu, D., Jensen, M. E., & Snyder, R. L. (2005). The ASCE standardized reference evapotranspiration equation.

Beguería, S., Vicente-Serrano, S. M., Reig, F., & Latorre, B. (2014). Standardized precipitation evapotranspiration index (SPEI) revisited: Parameter fitting, evapotranspiration models, tools, datasets and drought monitoring. *International Journal of Climatology*, 34(10), 3001–3023. <https://doi.org/10.1002/joc.3887>

Cantrell, L. (2023). *Mayoral Proclamation of emergency due to saltwater intrusion (2023-10953)*. Civil District Court for the Parish of Orleans. Retrieved from <https://nola.gov/next/mayors-office/news/articles/september-2023/2023-09-22-saltwater-intrusion/>

Christian, J. I., Basara, J. B., Otkin, J. A., Hunt, E. D., Wakefield, R. A., Flanagan, P. X., & Xiao, X. (2019). A methodology for flash drought identification: Application of flash drought frequency across the United States. *Journal of Hydrometeorology*, 20(5), 833–846. <https://doi.org/10.1175/jhm-d-18-0198.1>

Climate Hazards Center. (2024). CHIRPS: Rainfall estimates from rain gauge and satellite observations [Dataset]. Climate Hazards Center. <https://www.chc.ucsb.edu/data/chirps>

CO-OPS. (2024). CO-OPS 1-minute tsunami water level data [Dataset]. National Centers for Environmental Information. <https://doi.org/10.7289/V59884XF>

Ford, T. W., & Labosier, C. F. (2017). Meteorological conditions associated with the onset of flash drought in the Eastern United States. *Agricultural and Forest Meteorology*, 247, 414–423. <https://doi.org/10.1016/j.agrformet.2017.08.031>

Funk, C., Peterson, P., Landsfeld, M., Pedreros, D., Verdin, J., Shukla, S., et al. (2015). The climate hazards infrared precipitation with stations—A new environmental record for monitoring extremes. *Scientific Data*, 2(1), 150066. Data Descriptor. <https://doi.org/10.1038/sdata.2015.66>

Guidry, K., Guo, J., Goyal, R., & Hutchins, R. (2023). Preliminary estimates of the impacts of drought and excessive heat on Louisiana agricultural and forestry sectors, 2023 (pp. 2023–2066). Retrieved from <https://www.lsuagcenter.com/profiles/lblack/articles/page1701271994192>

Hobbins, M. T., Wood, A., McEvoy, D. J., Huntington, J. L., Morton, C., Anderson, M., & Hain, C. (2016). The evaporative demand drought index. Part I: Linking drought evolution to variations in evaporative demand. *Journal of Hydrometeorology*, 17(6), 1745–1761. <https://doi.org/10.1175/jhm-d-15-0121.1>

Hughes, A. L. H., Wilson, A. M., & Morris, J. T. (2012). Hydrologic variability in a salt marsh: Assessing the links between drought and acute marsh dieback. *Estuarine, Coastal and Shelf Science*, 111, 95–106. <https://doi.org/10.1016/j.ecss.2012.06.016>

Jankowski, K. L., Törnqvist, T. E., & Fernandes, A. M. (2017). Vulnerability of Louisiana's coastal wetlands to present-day rates of relative sea-level rise. *Nature Communications*, 8(1), 14792. <https://doi.org/10.1038/ncomms14792>

Liang, Y.-C., Lo, M.-H., & Yu, J.-Y. (2014). Asymmetric responses of land hydroclimatology to two types of El Niño in the Mississippi River Basin. *Geophysical Research Letters*, 41(2), 582–588. <https://doi.org/10.1002/2013GL058828>

Luo, X., Dee, S., Lavenhouse, T., Muñoz, S., & Steiger, N. (2023). Tropical Pacific and North Atlantic sea surface temperature patterns modulate Mississippi basin hydroclimate extremes over the last millennium. *Geophysical Research Letters*, 50(2), e2022GL100715. <https://doi.org/10.1029/2022GL100715>

McEvoy, D. J., Huntington, J. L., Hobbins, M. T., Wood, A., Morton, C., Anderson, M., & Hain, C. (2016). The evaporative demand drought index. Part II: CONUS-wide assessment against common drought indicators. *Journal of Hydrometeorology*, 17(6), 1763–1779. <https://doi.org/10.1175/jhm-d-15-0122.1>

Mo, K. C., & Lettenmaier, D. P. (2015). Heat wave flash droughts in decline. *Geophysical Research Letters*, 42(8), 2823–2829. <https://doi.org/10.1002/2015GL064018>

Mo, K. C., & Lettenmaier, D. P. (2016). Precipitation deficit flash droughts over the United States. *Journal of Hydrometeorology*, 17(4), 1169–1184. <https://doi.org/10.1175/JHM-D-15-0158.1>

Mo, K. C., & Lettenmaier, D. P. (2020). Prediction of flash droughts over the United States. *Journal of Hydrometeorology*, 21(8), 1793–1810. <https://doi.org/10.1175/jhm-d-19-0221.1>

Muñoz, S. E., & Dee, S. G. (2017). El Niño increases the risk of lower Mississippi River flooding. *Scientific Reports*, 7(1), 1772. <https://doi.org/10.1038/s41598-017-01919-6>

Muñoz, S. E., Dee, S. G., Luo, X., Haider, M. R., O'Donnell, M., Parazin, B., & Remo, J. W. F. (2023). Mississippi river low-flows: Context, causes, and future projections. *Environmental Research: Climate*, 2(3), 031001. <https://doi.org/10.1088/2752-5295/acd8e3>

NOAA. (2024). EDDI: Evaporative demand drought index [Dataset]. NOAA. <https://psl.noaa.gov/eddi/>

O'Donnell, K. L., Bernhardt, E. S., Yang, X., Emanuel, R. E., Ardón, M., Lerdau, M. T., et al. (2024). Saltwater intrusion and sea level rise threatens U.S. rural coastal landscapes and communities. *Anthropocene*, 45(1), 100427. <https://doi.org/10.1016/j.ancene.2024.100427>

Pendergrass, A. G., Meehl, G. A., Pulwarty, R., Hobbins, M., Hoell, A., AghaKouchak, A., et al. (2020). Flash droughts present a new challenge for subseasonal-to-seasonal prediction. *Nature Climate Change*, 10(3), 191–199. <https://doi.org/10.1038/s41558-020-0709-0>

Queen, W. H. (1974). Physiology of coastal halophytes. In R. J. Reimold & W. H. Queen (Eds.), *Ecology of halophytes* (pp. 345–353). Academic Press.

Ramseyer, C. A., & Miller, P. W. (2023). Atmospheric flash drought in the Caribbean. *Journal of Hydrometeorology*, 24(12), 2177–2189. <https://doi.org/10.1175/jhm-d-22-0226.1>

Rolando, J. L., Hodges, M., Garcia, K. D., Krueger, G., Williams, N., Carr Jr, J., et al. (2023). Restoration and resilience to sea level rise of a salt marsh affected by dieback events. *Ecosphere*, 14(4), e4467. <https://doi.org/10.1002/ecs2.4467>

Svoboda, M., LeComte, D., Hayes, M., Heim, R., Gleason, K., Angel, J., et al. (2002). The drought monitor. *Bulletin of the American Meteorological Society*, 83(8), 1181–1190. <https://doi.org/10.1175/1520-0477-83.8.1181>

Swenson, E. M., Evers, D. E., & Grymes, III, J. M. (2004). *Brown marsh task II.5, integrative approach to understanding the causes of salt marsh dieback: Analysis of climate drivers*. Louisiana Department of Natural Resources.

Turner, R. E. (2022). Variability in the discharge of the Mississippi River and tributaries from 1817 to 2020. *PLoS One*, 17(12), e0276513. <https://doi.org/10.1371/journal.pone.0276513>

Twine, T. E., Kucharik, C. J., & Foley, J. A. (2005). Effects of El Niño–Southern Oscillation on the climate, water balance, and streamflow of the Mississippi River basin. *Journal of Climate*, 18(22), 4840–4861. <https://doi.org/10.1175/jcli3566.1>

U.S. Geological Survey. (2024). National water information system [Dataset]. USGS. <https://doi.org/10.5066/F7P55KJN>

USGS. (2024). USGS 07374525 Mississippi River at Belle Chasse, LA. Retrieved from https://waterdata.usgs.gov/nwis/inventory/?site_no=07374525

vander Wiel, K., Kapnick, S. B., Vecchi, G. A., Smith, J. A., Milly, P. C. D., & Jia, L. (2018). 100-Year lower Mississippi floods in a global climate model: Characteristics and future changes. *Journal of Hydrometeorology*, 19(10), 1547–1563. <https://doi.org/10.1175/JHM-D-18-0018.1>

Vicente-Serrano, S. M., Beguería, S., & López-Moreno, J. I. (2010). A multiscalar drought index sensitive to global warming: The standardized precipitation evapotranspiration index. *Journal of Climate*, 23(7), 1696–1718. <https://doi.org/10.1175/2009jcli2909.1>

Visser, J. M., Sasser, C. E., Chabreck, R. H., & Linscombe, R. G. (2002). The impact of a severe drought on the vegetation of a subtropical estuary. *Estuaries*, 25(6), 1184–1195. <https://doi.org/10.1007/BF02692215>

Walker, N., Wiseman, J. W., Rouse, J. L., & Babin, A. (2005). Effects of river discharge, wind stress, and slope eddies on circulation and the satellite-observed structure of the Mississippi River plume. *Journal of Coastal Research*, 2005(216), 1228–1244. <https://doi.org/10.2112/04-0347.1>

Wiman, C., Hamilton, B., Dee, S. G., & Muñoz, S. E. (2021). Reduced lower Mississippi River discharge during the Medieval era. *Geophysical Research Letters*, 48(3), e2020GL091182. <https://doi.org/10.1029/2020GL091182>

Zhang, Y., & Hu, C. (2021). Ocean temperature and color frontal zones in the Gulf of Mexico: Where, when, and why. *Journal of Geophysical Research: Oceans*, 126(10), e2021JC017544. <https://doi.org/10.1029/2021JC017544>